Hybrid Propulsion of a Long Endurance Electric UAV

Tiago Miguel Moreira Ferreira
tmferr@msn.com

Instituto Superior Técnico, Lisboa, Portugal

November 2014

Abstract

The demand for alternative and clean power sources has been growing in the past years. The change to electric power can already be seen in the automotive industry, and the aeronautical industry is slowly following. The use of solar panels is a good alternative power source to use with electrical drives, since it is clean and readily and abundantly available. This thesis focuses on a system combining solar power generation and an electrical drive to power a 4.5 m span unmanned aerial vehicle for aerial surveillance over long periods of time. A solar-battery hybrid is a good solution for long endurance aerial vehicles, since there is a large area available on the wings to mount a solar array capable of supplying enough energy to maintain the aircraft airborne. The hybrid propulsion system will be tested and verified for energy and power availability versus mission requirements, since this is the main drawback of a solar system. Since these cells are to be mounted on a heat shrink film covered wing, and these cell tend to heat up, the behaviour of the film will be studied to verify the viability of the system assembly.The tests proved that the hybrid propulsion system is a feasible system, since the maximum output was 106 W, more than twice the energy required during the cruise phase. The film should be further tested on a test wing, since the 39.76% force decrease could induce serious changes to the geometry of the wing.
Keywords: Solar power, UAV, Hybrid propulsion, Electric flight, Long endurance

1. Motivation

For the last several years, environmental concern has grown due to the increasing proof supporting global warming. This concern, allied with the increasing costs of fossil fuels, has powered the search for alternative and clean energy sources.

One of the solutions is the use of solar power. The major problem in harvesting energy from the solar radiation is the efficiency of conversion from radiation to a energy form usable by today's technology. The most common available solar conversion technology, solar panels, have a efficiency of around 20%. Another limitation is the fact that the Earth rotates, so solar exposure is limited to during the day. Exposure is also reduced during cloudy weather. All these factors limit the application of solar power technology.

These limitations can be, somewhat, overcome with the use of hybrid systems, using solar panels to either accumulate energy or supply energy during low requirement situations, and an energy accumulator or backup power supply for peak power demand. These hybrid systems can enable a continuous functioning of the system.

In aviation this technology is also more useful due to the available area of the wings, on which is possible to mount solar panels, to supply energy to maintain flight. This could be used so that an aerial vehicle can remain airborne indefinitely, which is useful in reconnaissance or missions, such as aerial surveillance of forest zones during high fire risk season. Unfortunately the solar power technology is not yet advanced to maintain a usable manned air vehicle, due to the low efficiency of solar cells, but it is enough for use in Unmanned Aerial Vehicles (UAV). Due to recent evolution in processing capabilities and radio transmitters, and also in electric power and accumulation, UAVs are becoming more and more affordable and accessible. This makes the development of early warning and surveillance aerial systems a plausible reality.

2. Mission

This paper will focus on the hybrid aspect of the propulsion a long endurance unmanned aerial vehicle. The aircraft will be a Long Endurance Electric Unmanned Aerial Vehicle (LEEUAV) for use in civilian surveillance missions. The objective if to be an affordable platform, with off-the-shelf components, that can be easily deployed in locations with relative small space, while being able to carry a payload of up to 1 kg. As for the long endurance, it has to be able to gather, or generate, energy in mid flight to be able to stay airborne for long durations

of time, since the weight of the energy accumulators required for long duration flights would increase the take-off weight of the vehicle and reduced its payload carrying capabilities. The UAV is being developed for the LEEUAV project [6], and this thesis is a continuation of the Hector Vidalez MsC thesis [9]. In this project, the hybrid system has to be able to sustain a 8 hours flight, including take off and climb to an altitude of 1000 m. To achieve this result, the solar array, the energy accumulation and the whole hybrid system will be chosen and characterised to determine its capabilities. So several parameters of the energy supply and management systems, and the power requirement of the electric drive will be studied.

At the end of this project, the hybrid system must be able to supply enough energy to the power system, so that the mission can be accomplished.

Another aspect to be studied is the effect the heat from the solar array will have on the wing structure, which will be comprised of balsa and composite formers covered with a heat shrinking film, being that the main focus will be the effect of the heat in the covering film. The aircraft has to be tailored for the mission it has to accomplish. So in this section the mission requirements will be discussed.

3. Aircraft

The dimension of the aircraft is important for its mission, since it has to be large enough to accommodate all the systems and electronics, but small enough to be an affordable solution and to be able to deploy from small landing fields. The design of the aircraft was done in a previous paper.

For a high wing aspect ratio wing (>6), the most important aerodynamic factor is the aerofoil. Several low Reynolds number (Re) aerofoils were considered for the wing, but due to the specific requirements of the mission, an aerofoil was designed in house (Fig. 1).

Figure 1: LEEUAV aerofoil geometry obtained.

A 4.5 m wing span and 0.33 m mean wing chord was chosen as the design point for the project. A tailless design was also considered due to its superior aerodynamics and flight performance [3], but a conventional wing and tail design was chosen instead [5]. This allowed for a wing without sweep to accommodate the solar array and an inherently stable platform.

The relevant dimensions of the designed aircraft are summarized in Tab. 1.

Table 1: Relevant dimensions of the designed aircraft.

Span $[m]$	4.50
Root wing chord $[m]$	0.35
Tip wing chord $[m]$	0.25
Wing area$[m^2]$	1.50
Take-off weight $[kg]$	4.90

The aircraft was developed with the aid of a Computer Aided Design (CAD) system which allows the representation of the major components, enabling the verification of fitting and the study of the location of the various systems for functionality, weight distribution and ease of access. A rendering of the finished concept is shown in Fig. 2.

Figure 2: Rendering of the CAD concept.

Due to the long distance nature of the mission, the flight will be, on the most part of it, controlled by an autopilot, with a way-point feature, which means that the human controller at the ground station will define GPS coordinates which the autopilot installed on the aircraft will follow. As of yet, a human pilot will be required to take-off and land the aircraft.

4. Hybrid Propulsion

In the developed project, a long duration flight of a unmanned aerial vehicle was desired. The current energy accumulation technologies did not allow the storage of enough energy to sustain the model airborne over the course of the flight. For this reason, a hybrid propulsion UAV with two energy sources was designed.

The hybrid system would be accomplished by joining an energy accumulator, which would be charged prior to the beginning of the flight, and an energy production system. An array of solar cells was deemed the best option, since the wings have a large area, room to put the array was not a problem.

A scheme of the hybrid system can be seen in Fig. 3, and it will work in the following way: the energy in the accumulator will be used to take the UAV to the desired altitude, 1 km, and then transition to level flight at cruise speed. During the level flight,

the solar array will produce enough energy to power the motor and even recharge the accumulator in periods of excessive solar power.

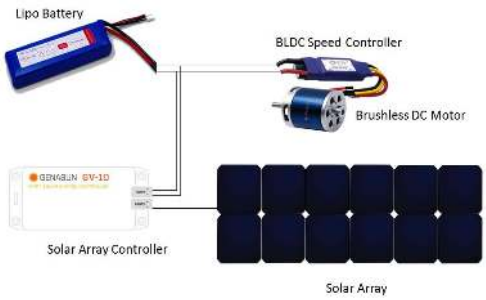

Figure 3: Scheme of the hybrid propulsion system for the LEEUAV

As it can be seen in Fig. 3, there is a solar array controller between the solar array and the batteries. This is a maximum power point tracker (MPPT), which enables the maximum power output from the solar array [4]. This MPPT also manages the charging of the LiPo batteries. As for the propulsion part of this system, the UAV will be propelled using the thrust produced by a out-runner brushless direct current (BLDC) electric motor which will spin a propeller.

The MPPT (maximum power point tracking) is an electronic device that varies the electrical operating point of the solar array to extract the maximum power possible.

As shown in Fig. 4, the voltage and current, and the power, extracted from a solar cell depends on the load put on it.

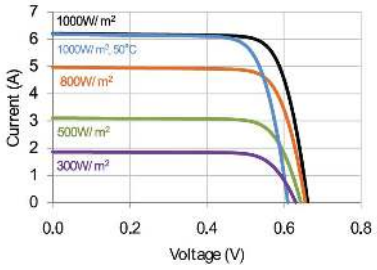

Figure 4: Tipical I-V curve for the C60 SunPower PV cell [8].

5. Solar Cells Testing

To validate the power curve (Fig. 4) supplied by the manufacturer of the PV cell, a simple experiment was devised.

Using a single PV cell, a variable load will be put in the electrical system, and the electrical parameters registered. The experiment will then be repeated with a solar panel, to verify that the behaviour is similar to that of a single cell. The variable load will be comprised by resistors connected in serial or in parallel.

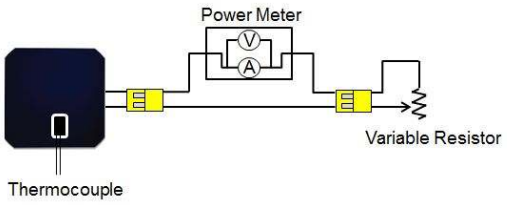

Figure 5: Single solar cell testing.

For the panel testing, it was decided to make two types of panel, a panel with association in series (Fig. 1(a)) and a panel with association in parallel (Fig. 1(b)), to check if the progression of the curve could be influenced by different electrical connections.

(a) Testing of three solar cells in series.

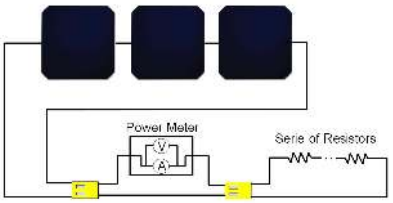

(b) Testing of three solar cells in parallel.

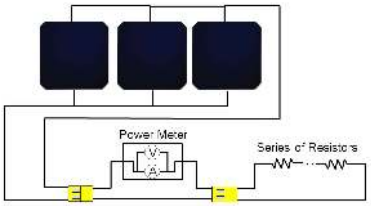

Table 2: Multiple PV cell test.

It was decided to go with only three cells in the panel test, since the results should be the same as with a higher cell count panel, the lower current output should allow for more available resistances.

Another test of interest is the power variation with the inclination of the solar array. As a model aeroplane usually achieves turns with over 40 banking, the inclination of the wing will directly influence the energy produced. To test this factor, the panels will simply be inclined towards the Sun, and the power output will be registered and plotted.

The temperature of the cells will also be tested, as this value will be needed during the film testing.

Due to the fact that some discrepancies can occur during the manufacture of the sensor, and to understand how accurate it can be, all the used sensors were calibrated when possible.

5.1. Single Cell Testing

The single cell test was repeated 4 times, at different times of the day, using 10 different loads to plot the curve. To measure the irradiation from the sun, a pyranometer was used. The whole irradiation measurement system was mounted on a wood board and can be seen in Fig. 6.

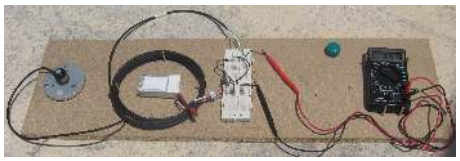

Figure 6: Solar irradiation measuring system.

The irradiation curve obtained using the pyranometer is shown in Fig. 7.

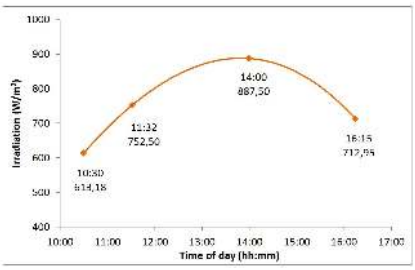

Figure 7: Times of the single cell tests and evolution of the solar irradiation during the day.

The results of the single PV cell test are shown in Fig. 8.

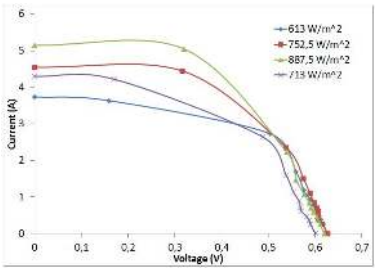

Figure 8: Single cell test.

When comparing these results with the curves supplied by the manufacturer (Fig. 4) the similarity is obvious. To further show the need of a MPPT, in Fig. 9 the power output of the several points were plotted, and show a clear peak power output. The MPPT will maintain the PV cell working around this maximum power point.

5.2. Efficiency Loss from Film Covering

The next experiments with the single cell were the film efficiency loss due to the covering of the heat shrinking film. The test was repeated on two different days and the results are shown in Tab. 3.

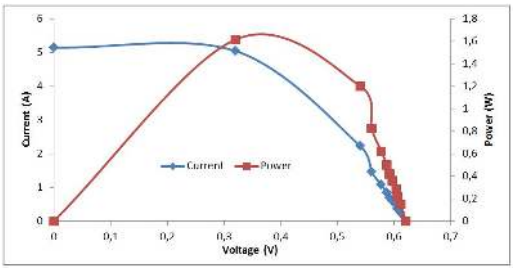

Figure 9: Evolution of the power output

Test 1	Irradiation (W/m^2)	Power (W)	Efficiency (%)
Clean	732.5	1.636	100.0
Yellow Film	732.5	0.971	59.3
Transparent Film	732.5	1.505	91.9
Test 2	**Irradiation (W/m^2)**	**Power (W)**	**Efficiency (%)**
Clean	802.5	1.710	100.0
Yellow Film	802.5	1.229	71.9
Transparent Film	800.0	1.609	94.1

Table 3: Results of the film variation experiment

Covering with the yellow film will not be an option because, with a power output loss of around 30%, it would make the system extremely inefficient, considering that on the full panel with 120 W output, there would be a 36 W loss. Using the transparent film will not be such a huge loss, but would negate the extra investment on a higher efficiency cell.

5.3. Efficiency Gains from Changing the Incidence Angle

The efficiency gain from directing the PV cell towards the sun, was tested on two separate days. The first measure was taken with the cell horizontal to supply a base line, and then repeated with the PV cell angled 25°and 45°towards the sun. The results of the tilting test can be observed in Tab. 4.

An average of 17.2% power gain was observed when the PV cell was tilted 45°towards the sun, which is now an unusual angle on a turning aeromodel, and a 4.4% gain was observed on the 25°test.These power gains were expected since since the irradiation from the sun arrives at a more perpendicular angle, reducing the losses from reflection.

Test 1	Irradiation (W/m^2)	Power (W)	Efficiency (%)
Horizontal	732.5	1.636	100.0
Tilted 45°	730.0	2.022	123.6
Test 2	**Irradiation (W/m^2)**	**Power (W)**	**Efficiency (%)**
Clean	802.5	1.710	100.0
Tilted at 25°	800.0	1.786	104.4
Tilted 45°	792.5	1.893	110.7

Table 4: Results of the tilt variation experiment

5.4. Multiple Cells Testing

For the multiple cell test (Fig. 10), the same measuring system was maintained, due to the same reasons as for the single cell, but also to maintain uniformity of the results.

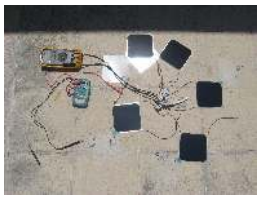

Figure 10: Circuit assembly used for the multiple cell tests.

For the series circuit, the results from the test are shown in Fig. 11.

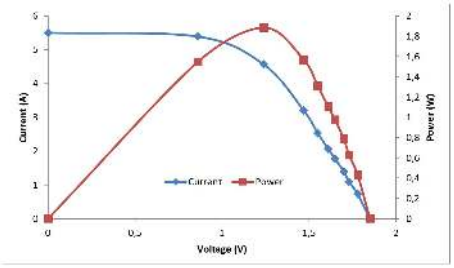

Figure 11: Test with three cells connected in series.

Similar procedure and results were obtained for the parallel circuit.

Since the objective of this test was to compare the output curve of the two circuits with the single cell, the Kirchhoff's current law (the sum of all the current flows entering a node is equal to all the current flows exiting the same node, Eq. 1) was used to convert the parallel curve to single cell current, and the Kirchhoff's voltage law (the sum of the voltage drop along a closed loop is equal to the total voltage drop of said loop, Eq. 2) was used in the series circuit to convert the voltage to the level

	Irradiation (W/m^2)	Power (W)
Test with 6 bulbs	897,5	105,75
Test with 5 bulbs	937,5	93,74

Table 5: Full array tests

of the single cell.

$$\sum_{i=1}^{n} I_{In_i} = \sum_{i=1}^{n} I_{Out_i} \tag{1}$$

$$\sum_{i=1}^{n} V_i = V_t \tag{2}$$

The resulting graph is shown on Fig. 12.

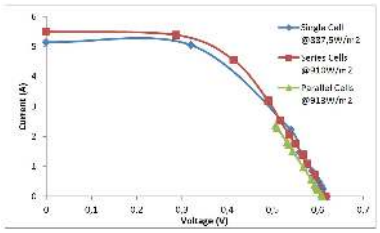

Figure 12: Curves of the single cell and the two circuits converted to single cell power.

As shown in Fig. 12, all three curves behave similarly.

5.5. Full Solar Array Test

To test the output power of the full array (Fig. 13), it was connected to light bulbs. The results of the two tests are presented in Tab. 5.

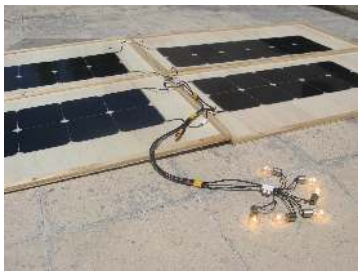

Figure 13: Full panel testing using light bulbs for load and a power meter for parameter measuring.

These maximum output power of the complete solar array is bellow the theoretical maximum power output of 137.4 W, for the six bulbs test. This can be explained by the decline of the efficiency of the solar array with the temperature, since during this test the solar array was around 60°C and the theoretical maximum power is obtain with the array at 25°C. Also, the load provided by the light bulbs might not be the maximum power point, which would also lower the output power of the solar array.

6. Testing of Other Components

The test of the MPPT will have the objective of knowing the efficiency of energy transfer from the solar array to the energy accumulator. A power meter will be placed between the solar array and the MPPT, and a second meter will be put between the MPPT and the battery. The power from before and after the MPPT will be compared, and the power efficiency calculated by Eq. 3.

$$\eta_{MPPT} = \frac{Power\ after\ MPPT}{Power\ before\ MPPT} \tag{3}$$

The test was conducted with the full hybrid system assembled, which means that the motor was providing a variable load on the system.

The results of the test are presented in Tab. 6.

	Power (W)
Before the MPPT	87.97
After the MPPT	78.15

Table 6: MPPT tests.

This resulted in an average 88.84% efficiency during the test, which is below the reported 92-96% efficiency.

7. Electric Motor Testing

To test the motor, an apparatus will have to be designed and built. As said before, the apparatus will consist of a swivel arm with the motor on one end and a load cell on the other.

The forces inflicted on the structured are calculated. The flying weight of the UAV is 48.12 N and the aerodynamic forces calculated in [9] are shown in Tab. 7.

Flight Phase	v (m/s)	L (N)	D (N)
Take off	4.91	23.80	0.95
Climb	7.29	48.47	2.48
Cruise	7.29	48.47	2.48
High Speed	20.66	50.42	11.49
Descent	10.44	48.37	2.67

Table 7: Aerodynamic forces during the different phases of the flight [9].

The maximum force needed of the motor comes in the high speed phase with the value of 11.49 N. A wood frame will be enough for this force requirement. The swivel arm will be made of a rectangular section steel beam, to prevent warping that could affect the readings. The final apparatus can be seen in Fig. 14.

The force measurement will be done with a Vishay model STC S-Type load cell, and the rotational speed of the motor will be measured with

Figure 14: Final apparatus for motor testing

the telemetry from the speed controller and entered manually for recording.

After the manufacturing and assembling of the testing apparatus (Fig. 14) , the load cell was calibrated.

Only three propellers were used in the test, a 10"x5", a 11"x5.5" and a 12"x6" from APC [1]. The first number is the diameter of the propeller and the second is its pitch, both in inches. The BLDC Motor used in this test was the Hyperion ZS 3025 10-Turn 775Kv [7]. The electronic speed controller used to control the speed of the BLDC motor was the Hyperion ATLAS 70A 4S [2]. The battery used was the Hyperion G3 VX 3S 4,200mAh.

Fig. 15 show the thrust obtained for the three different propellers.

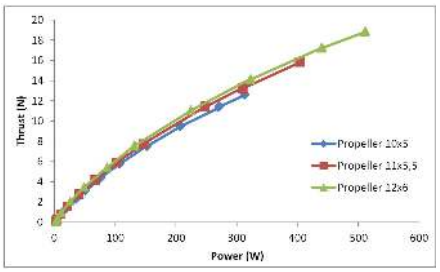

Figure 15: Thrust obtained by power consumed.

These results show that the larger the propeller, the higher the power consumed, but also the higher the output thrust. Also, for the same power input, the output thrust slightly increases with the increase of the propeller diameter.

As the objective of this test was to obtain the power required for each phase of the flight, a plot of the thrust versus power was done and a polynomial regression was done to obtain the equation for the power curve. This equation was then used to obtain the power necessary for each flight phase, which can be seen in Tab. 8.

In the take off and climb phase, the motor will be at maximum power because the aircraft has to accelerate to flying speeds and the motor has to input energy to the system so that it can increase its

Flight Phase	Drag (N)	10"x5" (W)	11"x5.5" (W)	12"x6" (W)
Take-Off	0.95	312.59	403.52	511.00
Climb	2,48	312.59	403.52	511.00
Cruise	2.48	39.53	36.89	33.45
Speed	11.49	273.63	252.20	237.78
Descend	2,67	0	0	0

Table 8: Power use for the different propellers to fulfil the thrust requirements.

altitude. In the cruise phase the power requirement is bellow the 50 W calculated in [9], and well bellow the 153 W maximum theoretical power of the solar array. In the speed phase, all the tested propellers consumed more than 153 W, but this is a phase that will not be much used, so the battery will supply the extra power required.

8. Complete Hybrid Propulsion System

8.1. Complete System Test

For the full system testing, the two six by two solar panels and the two five by two panels were connected to the MPPT. The other components were described in Sec. 7, where a 10"x5" was chosen. A schematic of the complete hybrid system can be seen in Fig. 16.

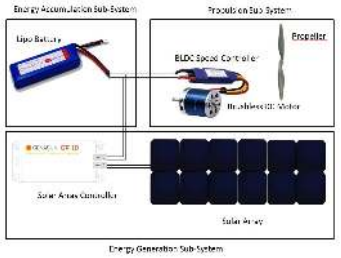

Figure 16: Schematic of the complete hybrid propulsion system.

The power meter only measures current one way, so if the current flow is opposite the measured way, it will show as 0 A. The power output of the battery and the MPPT can be seen in Fig. 17.

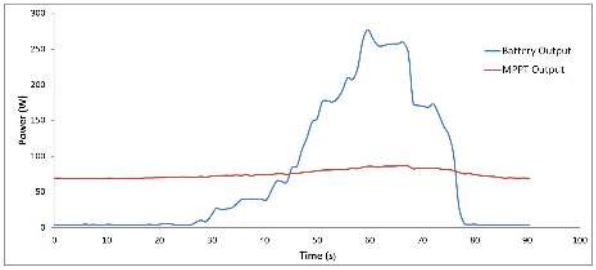

Figure 17: Power output of the battery and MPPT during the full system test.

The first noticeable result is that the MPPT always supplies approximately the same power, and the battery only supplies power when needed. On Fig. 17, the motor began throttling up on the 15 s mark, and the battery only started supplying power at the 25 s mark. This means that during 10 s, the MPPT was powering the motor and the excess power was recharging the battery. This result is not directly observable in the result graph due to the fact that the power meter does not measure "negative" current, so if the current flows in the opposite way, it outputs a 0 A measure. This evidences that if the available power from the solar array is lower than the power required by the motor, the excess power will charge the battery, and when the power supplied by the solar array is not lower than the power required by the propulsion sub-system, the lacking power will come from the battery, thus discharging it.

The other noticeable result is that the maximum output of the MPPT, even at full load, was 86.55 W, which is well under the 153 W maximum theoretical power output of the solar array. This could be due to the fact that the MPPT raises the output current with decreasing voltage, as can be seen in Fig. 18, or this can be a result of the power curve of the solar array itself since the MPPT is managing the charging voltage of the LiPo battery, which needs to be charged at constant voltage and constant current.

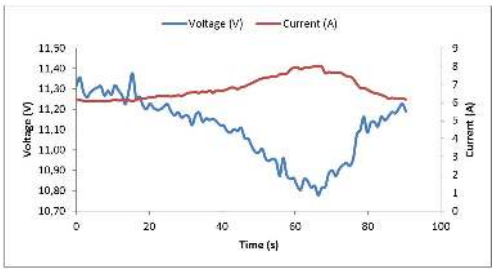

Figure 18: Plot of the current and voltage output of the MPPT during the full test

8.2. Mission Simulation

A mission simulation test was done, where the motor was ran at full throttle for ten minutes and then the throttle was reduced until the power consumed by the motor was 50 W, emulating the power required during the cruise phase of the mission. This cruise phase was maintained until the battery was considered spent. The test was done using the 11"x5.5" APC propeller, since this was the one that had the closest power requirement to the mission parameters (Sec. **??**). This test did not fully emulate the conditions of the mission as there will be air flowing over the solar array cooling it, but since the PV cells efficiency decreases with the rise of tem-

perature, the error in these testing conditions is on the side of safety. For this test both of the 4,200 mAh batteries will be used, as just one will not have enough energy for the 10 minutes full power motor run.

The test ran for 6 hours and 47 minutes, and the results of this test are shown in Fig. 19. As can be noted the conditions during the day were not ideal, being the day of the test later than the mission specified, and high altitude thin clouds were present throughout the day, resulting in a lower and more inconstant than expected irradiance, being the maximum 634.8 W/m^2. Despite these conditions, the energy generation sub-system supplied over half the power required during the cruise phase, having a 70 W maximum output, at an average 16.22% efficiency and 35.1 °C temperature. During the climb phase simulation, the motor consumed 6,554.4 mAh, which is 78% of the capacity of the combined batteries.

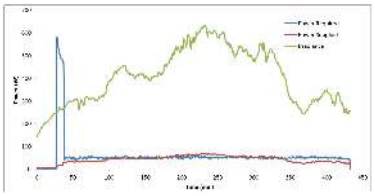

Figure 19: Hybrid propulsion system mission simulation.

9. Heat Shrink Film Test

Due to the fact that the wing skin is a heat shrinking film, that will have to support the solar cell array, which is comprised of dark grey coloured solar cells, some problems of warping can occur on the wing because the solar cells will heat up, causing a rise in temperature of only the top skin, as the bottom skin will be in the shadow of the solar array.

9.1. Testing Apparatus

To better understand the behaviour of this film, a testing apparatus was designed. The device was designed to allow the assembly of a solar cell on top of a strip of film, although the characterization will be done with a more controllable heat source.

The apparatus was designed to measure the force due to the shrinking film when subjected to a heat source. To measure the force, a strain gauge will be used. The testing device will be a frame, where the film will be fixed on one side of the frame, and the other side will be fixed to a moving bar that is hold by a metal sheet, which will have the strain gauge mounted on to it to measure it's strain.

The final geometry is shown in Fig. 20.

The strain gauge needs, at least, a 6 mm wide plate for the measuring portion of it to be bonded

Figure 20: Final geometry of film testing apparatus.

on the part it will be measuring, the width of the load cell will be 6 mm, to maintain its section as small as possible. The built load cell is shown in Fig. 21.

Figure 21: Built aluminium load cell with the strain gauge.

To control the temperature applied to the film the Joule's first law was employed. So a simple grid made with nickel chrome wire was designed, as seen in Fig. 22.

Figure 22: Heating element used in the heat shrink film test.

First, the film was heated up to 120°C, and the load exerted by the shrinking was recorded over time. Then the film was left to cool down to room temperature. This simulated the application of the covering film to the wing of the model. Then the film was reheated to 60°C simulating the thermal load during the use of the solar array.

The output from the strain indicator used to read the output from the load cell was in micro extension,$\mu\varepsilon$, so in order to obtain the load exerted by the film, the formulas shown on Eq. 4 were used.

$$\sigma = E_{aluminium} \times \varepsilon \times 10^{-6} F = \sigma \times area_{crosssection} \quad (4)$$

Since the test specimen is 0.5 mm thick and 6 mm wide, its cross section area is 3 mm^2.

9.2. Experimental Results

The experimental setup is illustrated in Fig. 23. In the first test, the temperature was taken with

the infrared thermometer, but this proved unreliable, since the film is semi transparent and the thermometer would pick up the temperature of the heating element. The following tests were conducted using the thermocouple. The value was read in the strain indicator and on the screen of the computer with the DAQ board, and written together. The temperature measured from the thermocouple was recorded for posterior analysis since it also recorded time.

Figure 23: Heat shrink film test montage.

After the linear response verification, the heat test was conducted. One test with the infrared thermometer and four tests with the thermocouple were done. Due to the limitations of the infrared thermometer, the reheating part of the test was only done using the thermocouple. Also, due to difficulties, the infrared thermometer test had no time recording. The results of the thermocouple tests can be seen in Fig. 24.

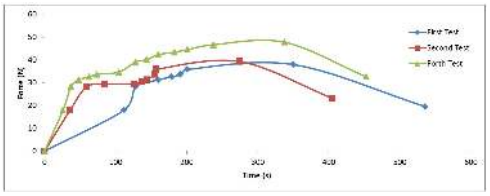

Figure 24: Heat shrink film force tests with the thermocouple.

Due to the inconsistency of the heat produced by the nickel chrome wire grid, the results vary with the position of the apparatus on top of the heat grid, even with positioning caution. This is evident in the time difference between the various tests, and, also, on the maximum force of the fourth test, which actually even over heated and punctured. On the third test the film slipped from the apparatus, thus that test was invalidated. Despite the inconsistencies, this test yielded interesting results. As was foreseen, the heating of the film increases the force it produces, up to an average maximum force of 39.46 N. The first interesting result is that the heat shrink film increases the force during cooling, due to the heat expansion phenomenon in which the material expand with increase temperature and contract with decreasing temperature. This effect allow for the maximum force after cooling to be, on average of the three test, 41.70 N, a 5.6% increase of force. The other interesting result is the force decrease when the heat is reapplied due to the same phenomenon of heat expansion. The heat might not be enough to cause the shrinking of the film, and the heat expansion prevails. At reheating the force decreases to, on average of the three tests, 25.12 N, a 39.76% force decrease.

10. Conclusions

The objective of this thesis was to design and evaluate a hybrid propulsion system for a long endurance electric unmanned aerial vehicle (UAV). For the accomplishment of this objective, the mission objectives and requirements were defined and explained, and a UAV design was proposed and evaluated. The performance of this UAV were then used to calculate the required energy requirements for the successful completion of the mission.

A hybrid system comprised of photovoltaic solar cells (PV cells), assembled in an array, and a lithium polymer (LiPo) battery was deemed the best solution, since the LiPo battery has a high energy density (can accumulate large amounts of energy for its weight), and the large area available on the wings are a suitable place to mount a solar array of sufficient capacity to supply energy during the cruise phase of the mission. To verify the validity of this system, several tests were conducted.

The first test focused on the individual cells, to validate the load curve supplied by the manufacturer, to create the load curve. The result curve was closely matched with the supplied curve. The test was repeated with different PV cell circuits to verify the curve characteristics remained with different PV cell configurations. The next test was to test the individual cell with energy input variations by changing the angle of incidence of the light on the cell, in which an energy gain was achieved, and using the UAV covering film over the cell, which resulted in energy output losses. The tilting test resulted in an average 17.15% increase in power output during the 45 test. The covering film test resulted in an average decrease of 34.4% and 7% power losses during the yellow and transparent films test, respectively.

A full array test was then conducted to verify the maximum power the array could supply, and it achieved 105.75 W. Then the full array was connected to the rest of the hybrid system, the MPPT, the battery and the motor. During this test the efficiency of the MPPT and the operation of the full system were studied. The MPPT achieved a 88.84% average efficiency. The full system worked in a surprising way, where energy would only be drawn from the battery when the needed power required exceeded the MPPT output, and the power output from the MPPT varied with the voltage of the battery, so the more depleted the battery the

higher the output of the MPPT.

Despite the less than ideal conditions, the mission simulation test was considered a success, since the test ran for 6 hours and 47 minutes with less than 630 W/m^2 irradiation, where the energy generation sub-system had a maximum output of 70 W and an average efficiency of 16.22% at an average 35.1 °C, while supplying over half the power required during the cruise phase.

In conclusion, the mission should be a success due to the fact that the simulation was almost successful despite less than ideal conditions. To allow the analytical prediction of the flight time, the dependence of the temperature of the solar panel, and therefore the efficiency, with the solar irradiation should be studied further.

Due to the construction method of the UAV, heat shrinking film over a balsa frame, a test on the behaviour of the covering film was conducted to ascertain the viability of the mounting of the solar array on the wings. For this purpose of testing the film, a steel frame and aluminium load cell were designed and built. A heating element was also designed and build to enable the control of the heat applied to the film. The behaviour of the film was unexpected since the film would contract during the heating phase, and continue to contract after the heat was turned off, but when heat was reapplied, it would extend. The conclusion derived from these results is that further test should be done since the warping of the wing is not intuitive. The relaxation of the top cover film can be a good thing, since this relaxation promotes the decrease of the dihedral of the wing, counteracting the lift force on the wings, decreasing the bending of the wing. On the other side, decreasing the dihedral of the wing also decreases the rolling stability of the UAV. Besides decreasing the dihedral, some warping of the wing can also occur, which could change the flight characteristics, mainly drag and stall characteristics, which could significantly affect the mission.

In the future, a better and more accurate test of the motor will be done. This will allow the choice of the best motor and propeller combination for the flight envelope of the mission. This test will be done in a wind tunnel, which will allow the closer simulation of the flight variables.

As for the system assembly, a partially built wing with a heating element under the skin should be put on the wind tunnel to ascertain the temperature of the film with the airflow, and to determine if the warp of the wing is significant enough to change the flight characteristics of the UAV. If this proves true, a new method of building the wings may prove needed, or a different way to mount the solar array on the wing to reduce the heat transfer.

Acknowledgements

I would like to thank my parents, Gracinda Ferreira and Mário Ferreira, for supporting me along my academic path. I would also like to thank Daniela Carvalho for always being there to help me along the way.

Thanks to the professors, Dr. André Marta and Dr. Virginia Infante, that guided me and helped me during the making of this thesis. And also thanks Diogo Rechena for the help in spell checking and proof reading.

References

[1] APC. `http://www.apcprop.com/v/index.html`. Acessed in March 2014.

[2] H. S. Controler. `http://www.hyperion-world.com/products/product/HP-ATLAS-070LB`. Acessed in March 2014.

[3] H. Karakas, E. Koyuncu, and G. Inalhan. Itu tailless UAV design. *Journal of Intelligent and Robotic Systems*, 69(1-4):131–146, 2013.

[4] Z. Lei and H. Kawamura. Design and flight test of a solar-powered unmanned air vehicle for long endurance, 2014. Tokio University of Science, Suwa.

[5] A. C. Marta. Long endurance electric uav, research line of aeronautics and space. Technical report, IST, 2013.

[6] A. C. Marta and P. V. Gamboa. Long endurance electric uav for civilian surveillance missions. Technical report, LAETA, CCTAE, Instituto Superior Tcnico and Universidade da Beira Interior, 2014.

[7] H. Motor. `http://www.hyperion-world.com/products/product/HP-ZS3025-10`. Acessed in March 2014.

[8] SunPower. SunPower's C60 solar cell mono cristalline silicon characteristics pamphlet.

[9] H. M. G. Vidales. Design, construction and test of the propulsion system of a solar uav. Master's thesis, IST, March 2013.